Escherichia coli Phosphoenolpyruvate Dependent Phosphotransferase System. Copurification of HPr and α1–6 Glucan†

G. Dooijewaard, F. F. Roossien, and G. T. Robillard*

ABSTRACT: A rapid, high-yield procedure has been developed for the purification of HPr from the *Escherichia coli* phosphoenolpyruvate dependent phosphotransferase system. During this procedure, the protein copurifies with a 2500-dalton homopolysaccharide which we have identified as α1–6 glucan. The results of steady-state kinetic measurements of the phosphotransferase activity demonstrate that the polysaccharide works as an activator of the phosphotransferase system probably at the level of the HPr:P-E_I complex or the P-HPr:E_{II} complex.

The phosphoenolpyruvate dependent hexose transport system is, relative to the number of macromolecules involved, a rather simple, energy-dependent, transport system. As characterized by Roseman and co-workers (Roseman, 1969) the system is composed of one soluble carrier protein, HPr, one soluble enzyme, E_I, and a membrane-bound complex, E_{II}. It catalyzes the following reactions.

$$\text{PEP}^{1} + \text{HPr} \xleftrightarrow[\text{Mg}^{2+}]{E_I} \text{P-HPr} + \text{pyruvate}$$

$$\text{P-HPr} + \text{hexose (out)} \xleftrightarrow[\text{Mg}^{2+}]{E_{II}} \text{hexose-P (in)} + \text{HPr}$$

Variations on this basic system have been found in *Escherichia coli* and other microorganisms (Saier, 1977; Postma & Roseman, 1976; Cirillo & Razin, 1973), but the elements stated above are common to all these systems. The apparent simplicity of this system makes it an attractive candidate for detailed physical–chemical studies of the transport process. Many physical techniques, however, demand large quantities of material for measurements. For this reason, we have focused our attention, initially, on developing high yield, rapid purification procedures for HPr and E_I (Robillard et al., 1979). During the course of the isolation, losses in HPr were encountered which were larger than expected for a single purification step, as judged by PTS activity measurements. Closer investigation has shown that these apparent losses result from the decrease in "specific activity" of HPr upon removal of an α1–6 glucan polysaccharide. This polysaccharide functions as an effector of the PTS.[1] The copurification, characterization, and kinetic studies are reported below.

Bacteria. E. coli K235 have been grown to mid-exponential phase in a commercial 3000-L fermentor on a glucose–salt medium (Kundig & Roseman, 1971a). After harvesting, the cells were washed with 1% KCl, centrifuged, and stored as a frozen cell paste at −20 °C until use. The ptsH, ptsI, and ptsHI mutants were *Salmonella typhimurium* strains SB2226, SB1690, and SB2950, respectively, obtained from Dr. P. Postma (1976), B.C.P. Jansen Institute, University of Amsterdam. They were grown in 7.5 mM $(NH_4)_2SO_4$, 0.4 mM $MgSO_4$, 60 mM K_2HPO_4, and 33 mM KH_2PO_4 containing 0.2% galactose and 20 mg/L tryptophan.

Measurements of the Phosphotransferase Activity. HPr "activity" was measured by using methyl α-D-[U-^{14}C]-glucopyranoside as the phosphate acceptor and a crude cell extract of the ptsH mutant, SB2226, as the source of E_I and E_{II} or pure E_I (see Robillard et al., 1979) and a partially purified E_{II} preparation (Postma, 1976) from the ptsHI mutant SB2950. The assay procedure used has been described previously (Kundig & Roseman, 1971b). Methyl α-D-[U-^{14}C]glucopyranoside (180 mCi/mmol) was purchased from The Radiochemical Centre, Amersham. Phosphoenolpyruvate (monocyclohexylammonium salt) was purchased from Sigma. All other chemicals were analytical grade reagents.

Sugar Determination. The presence of sugar was detected by using the orcinol–sulfuric acid method (Winzler, 1955). The concentration of sugar was determined by comparison with a standard solution of glucose analyzed by the same procedure.

Inorganic phosphate was detected by using the ammonium molybdate procedure of Fiske & SubbaRow (1925).

Protein was determined by the method of Lowry et al. (1951).

NMR spectra were obtained on a Bruker HX 360-MHz spectrometer operating in the Fourier transform mode. All spectra were recorded at 305 K. Proton spectra at 360 MHz were recorded on samples in 5-mm cylindrical microcells (Wilmad) by using a pulse repetition rate of 1.7 s. ^{13}C natural abundance NMR spectra were collected at 90.5 MHz in the quadrature detection mode by using 10-mm tubes containing a microcell insert (Wilmad). The chemical shift relative to Me_4Si was determined by using a sealed capillary containing Me_4Si. Decoupled spectra were collected with broad-band noise decoupling (5 W) and a pulse repetition rate of 35 s. Proton coupled spectra were recorded by using gated decoupling between data acquisition to preserve the nuclear Overhauser enhancement. ^{31}P NMR spectra were collected at 145.7 MHz on the same samples employed for ^{13}C NMR spectra. No proton decoupling was used. The pulse repetition rate was 30 s. All spectra were collected by using a D lock on the D_2O signal of the solvent.

HPr Isolation. HPr was isolated by a simplification of the procedure of Anderson et al. (1971; the purification from unheated crude cell extract). The following modifications were made: (1) the DEAE-cellulose column was eluted with a 6-L linear gradient of 0–100 mM KCl in 10 mM Tris-HCl buffer, pH 7.6; (2) concentrating and desalting steps were performed on an Amicon ultrafiltration apparatus equipped with a UM 2 membrane; (3) the CM-23 and Sephadex G-10 columns

† From the Department of Physical Chemistry, University of Groningen, Paddepoel, Groningen, The Netherlands. *Received January 22, 1979.* This research and the 360-MHz NMR facility at the University of Groningen have been supported by the Netherlands Foundation for Chemical Research (S.O.N) with financial aid from the Netherlands Organization for the Advancement of Pure Research (Z.W.O.).

[1] Abbreviations used: PTS, phosphotransferase system; PEP, phosphoenolpyruvate; Me_4Si, tetramethylsilane; DSS, 2,2-dimethyl-2-silapentane-5-sulfonate; αMglc, methyl α-D-glucopyranoside; $NaDodSO_4$, sodium dodecyl sulfate; ptsH, ptsI, and ptsHI, mutants lacking HPr, E_I, and HPr plus E_I, respectively; Sephadex, registered trademark of Pharmacia Fine Chemicals.

0006-2960/79/0418-2990$01.00/0 © 1979 American Chemical Society

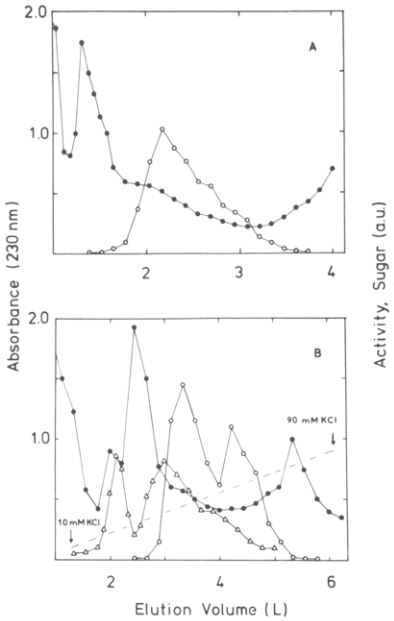

FIGURE 1: DEAE-cellulose chromatography of the protamine sulfate treated crude cell extract with (A) batchwise elution as described (Anderson et al., 1971) and (B) gradient elution which uses a linear gradient from 0 to 100 mM KCl (6 L total). Absorbance (230 nm) (●—●); HPr concentration (○—○); sugar concentration (△—△); KCl concentration (---). Measurements were made as described under Materials and Methods.

Scheme I

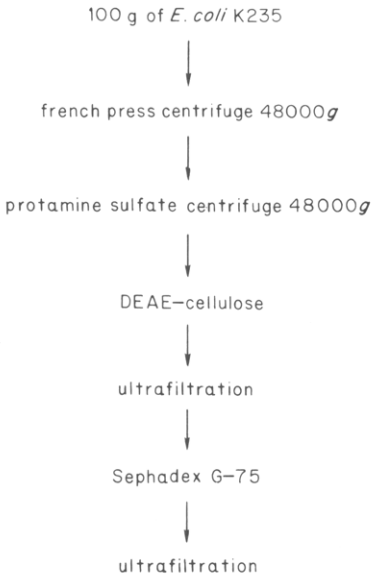

were omitted. The isolation procedure is summarized in Scheme I. Further data are presented under Results.

Results

Isolation of HPr. Figure 1 shows the elution profile of the supernatant of the protamine sulfate step in Scheme I on DEAE-cellulose under two conditions. On batchwise elution (Figure 1A) as used by Anderson et al. (1971), HPr elutes after the major absorption peaks in a broad zone apparently consisting of several overlapping peaks. Gradient elution (Figure 1B), which results in a more highly resolved chromatogram, shows two peaks of HPr concentration eluting at 45 and 60 mM KCl, respectively. The HPr-containing fractions in Figure 1A were pooled as a single peak, those in Figure 1B as two separate peaks. The three preparations of partially purified HPr were concentrated by ultrafiltration and

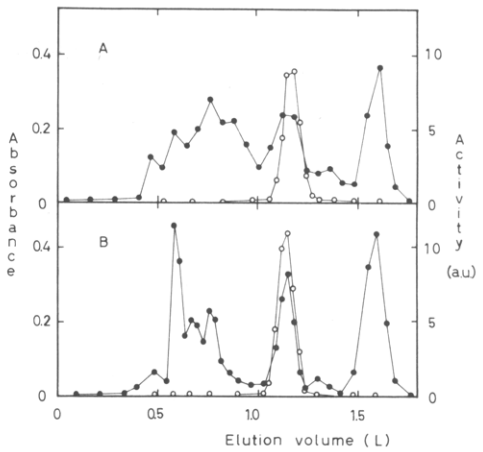

FIGURE 2: Sephadex G-75 chromatography of the HPr pool from the DEAE-cellulose chromatography in Figure 1A (A) and of the recombined HPr pools in Figure 1B (B); each pool was concentrated without NaN_3. Absorbance (230 nm) (●—●); HPr concentration (○—○). Measurements were made as described under Materials and Methods.

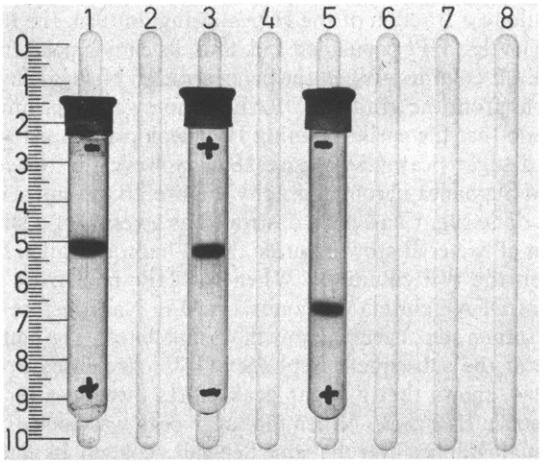

FIGURE 3: Standard polyacrylamide disc gel electrophoresis of pure HPr obtained from the Sephadex G-75 chromatography in Figure 2B. (1) Fifteen percent polyacrylamide gels at pH 9.5; (3) 15% polyacrylamide gels at pH 4.5; (5) 15% polyacrylamide gels at pH 9.5 in the presence of $NaDodSO_4$. The protein was stained with Coomassie Brilliant Blue.

chromatographed on Sephadex G-75. The elution patterns showed a single peak of HPr at a molecular weight of 9500 irrespective of the HPr peak chromatographed. Moreover, the two preparations from Figure 1B, chromatographed either separately or recombined into one preparation, gave identical profiles of absorption and HPr concentration, showing that, on Sephadex G-75, there is no difference between the various HPr peaks from DEAE-cellulose. Some of these results are presented in Figure 2. The preparation from the batchwise DEAE elution is not yet pure (see Figure 2A); the absorption profile is asymmetric and much broader than the HPr peak. With the recombined preparation from the gradient DEAE elution, however, the symmetric profiles of the 230-nm absorption and HPr concentration clearly coincide (see Figure 2B), suggesting that the protein is pure. This is confirmed by polyacrylamide gel electrophoresis of the pooled peak which shows a single band on pH 9, pH 4, and $NaDodSO_4$ gels (see Figure 3). The yields of HPr by this procedure will be treated, in detail, further on.

Copurification of a Polysaccharide. The two HPr peaks from the gradient DEAE elution, Figure 1B, do not result from two types of HPr with differing charge or size. The purified

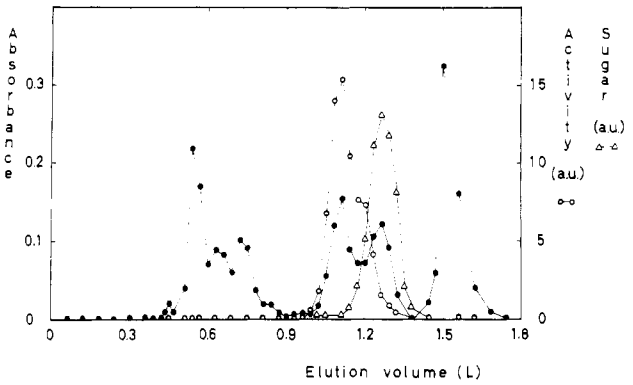

FIGURE 4: Sephadex G-75 chromatography of the recombined HPr pools, from Figure 1B, concentrated in the presence of 1 mM NaN_3. Absorbance (230 nm) (●—●); HPr concentration (○—○); sugar concentration (△—△). Measurements were made as described under Materials and Methods.

peaks are identical in these properties as shown on subsequent Sephadex chromatography and polyacrylamide gels. The two peaks could signal, however, a specific binding of some molecule to a fraction of the HPr altering, in turn, the total charge on that HPr population and, thus, its elution point from the DEAE column. When the concentration of sugar in the fractions from the gradient DEAE elution was determined, we found that the earliest eluting HPr peak overlapped with a broad sugar peak (see Figure 1B). However, in the subsequent Sephadex chromatography, Figure 2B, no sugar was found. The sugar had been destroyed as a result of a small amount of bacterial growth during the 48-h ultrafiltration step between the two columns. When the HPr pool from the gradient DEAE elution was made 1 mM in NaN_3 before the concentration step, bacterial growth was inhibited. The elution profile of the subsequent Sephadex G-75 chromatography, Figure 4, shows that a sugar peak elutes directly after an asymmetric HPr peak. When the sugar peak was pooled and rechromatographed over the same Sephadex column, its elution point was unchanged. This isolation procedure yields 50 μmol of sugar per 100 g of *E. coli* wet cell paste.

Characterization of the Polysaccharide. (*1*) *Chemical Composition.* Coupled gas chromatography and mass spectral analysis showed that the sugar polymer was composed, exclusively, of D-glucose units. Inorganic phosphate analysis was unable to detect phosphate in the polymer above 0.1 mol of P_i/mol of glucose. Similar negative results were obtained with ^{31}P NMR measurements.

(*2*) *Molecular Weight.* The point of elution of the sugar peak from Sephadex G-75 has been used to approximate its molecular weight. It is equivalent to the point of elution of dextran polymers with a molecular weight of 2500. This corresponds to a polysaccharide 15 glucose units in length.

(*3*) *Structure Analysis.* Figure 5 presents the natural abundance ^{13}C NMR spectra of the polysaccharide in Tris buffer. The decoupled spectrum, Figure 5A, shows that all units are in the same configuration, either α or β, resulting in a single resonance for each carbon atom. If both α and β anomers were present, two sets of resonances would be observed with relative intensities reflecting the relative populations of the anomers. In the proton coupled spectrum, Figure 5B, the peak at approximately 68 ppm which splits into a triplet is assigned to the glucose 6 carbon (see Figure 6, inset). The splitting arises from coupling to the two methylene protons. The resonance of the 6 carbon in glucose monomers or polymers with 1–4 glycosidic linkages occurs at higher fields, approximately 62 ppm (Jennings & Smith, 1973). The shift

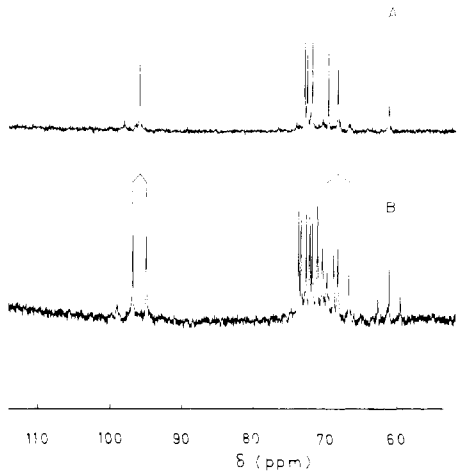

FIGURE 5: The 90.5-MHz natural abundance ^{13}C NMR spectra of α1–6 glucan. (A) Broad-band noise decoupled, 10000 accumulations; (B) proton coupled, 12000 accumulations. The resonance at 62 ppm is due to Tris.

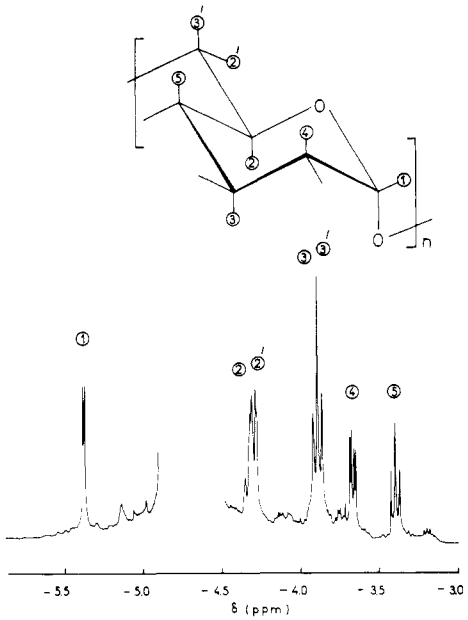

FIGURE 6: The 360-MHz ^1H NMR spectrum of α1–6 glucan. The numbers above the peaks represent the protons of the pyranose ring (see inset) resonating at the indicated field position.

downfield is caused by formation of a glycosidic bond with the 6 carbon. The resonance at 96 ppm, which splits into a doublet in the coupled spectrum, is assigned to the 1 carbon. In an α1–4 linkage, this resonance occurs downfield of 100 ppm, while in an α1–6 linkage it occurs upfield of 100 ppm (Jennings & Smith, 1973).

The simplicity of the ^1H NMR spectrum of this polysaccharide also indicates that all units are in the same configuration. The position of the anomeric proton resonance at −5.4 ppm is consistent with an α-anomer configuration. Thus, the isolated polymer is a homopolymer of D-glucose constructed entirely from α anomers via 1–6 glycosidic linkages.

Conformation of the Polysaccharide. Further studies of the proton NMR spectra reveal details of the configuration of the polymer. An intensity of seven protons is present in Figure 6, one proton each in resonances 1, 4, and 5 and two protons each in resonances 2 and 3. The numbers above the peaks indicate which protons in the structural formula resonate at the various spectral positions. These assignments have been made via selective decoupling experiments as shown in Figure

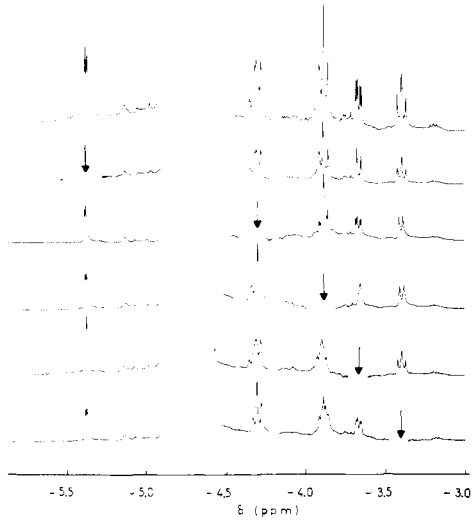

FIGURE 7: The 360-MHz ^{1}H NMR spectra of α1–6 glucan during selective decoupling. The frequency of irradiation is marked by an arrow in each spectrum.

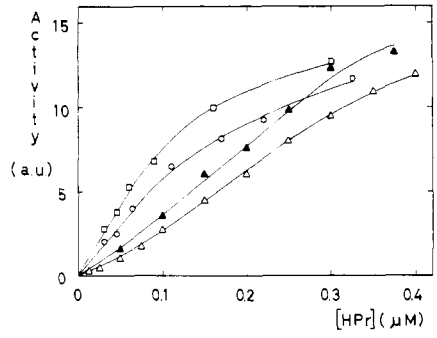

FIGURE 8: Measurements of the rate of αMglc phosphorylation (activity) as a function of HPr concentration for HPr from the various stages of the isolation procedure. Crude cell extract (□—□); DEAE pool (○—○); Sephadex G-75 pool (△—△); Sephadex G-75 pool recombined with a saturating amount of α1–6 glucan just before assaying (▲—▲). The activities, expressed in arbitrary units, were determined in the presence of a fixed amount of E_I and E_{II}, by using 50 μL of the crude cell extract of the mutant SB2226, containing 500 μg of protein. The activities were obtained from time-dependent plots and represent the initial rate of phosphorylation in the steady state. The concentration of HPr in the Sephadex G-75 pool was determined by Lowry's method; the concentration of HPr in the crude cell extract and the DEAE pool was computed as described in the Discussion.

7. In this figure, only one small coupling (≈3 Hz) is present, between protons 1 and 4, indicating that they are in an axial–equatorial arrangement. The remainder of the couplings are large (10 Hz) corresponding to axial–axial couplings as shown in Figure 6, inset. For proton 2 to be axial relative to proton 3′ requires that the glycosidic linkage have the same configuration as the α1–4 linkage of amylose (Greenwood, 1970). Thus, it is possible for this α1–6 glucan to form the same type of helical structures found for the amylose helix. However, the parameters of the helix will be different.

Role of α1–6 Glucan in the PTS. Since α1–6 glucan copurifies with HPr and the elution patterns from the DEAE-cellulose and Sephadex G-75 columns could be interpreted as indicating a binding between these two molecules, we have tested whether α1–6 glucan effects the PEP-dependent phosphotransferase activity. The phosphotransferase activity was measured as a function of HPr concentration at fixed concentrations of E_I and E_{II}. Figure 8 presents the results of these measurements for HPr taken from various stages in the purification procedure. All plots show saturation behavior as expected, HPr being a substrate of the PTS (Postma & Roseman, 1976). The shape of the curve, however, differs markedly, depending on whether HPr is in a stage of isolation where the preparation is rich in α1–6 glucan or not. HPr in the sugar-containing preparations yields curves approximating a hyperbola; the pure HPr yields a sigmoidal shaped curve. Recombination of pure HPr and α1–6 glucan just before assaying the phosphotransferase activity restores the hyperbola (see Discussion). The same results are obtained whether the PTS activity is measured by using a ptsH mutant cell extract as the source of E_I and E_{II} or pure E_I and a partially purified E_{II} membrane fraction. The interpretation of these results is presented below.

Scheme II

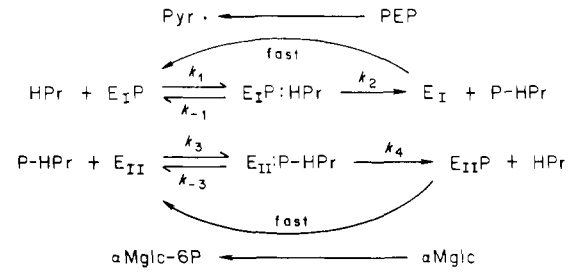

Discussion

Relationship between Phosphotransferase Activity and the Concentration of the PTS Components: Theoretical Treatment. The relative concentration of the PTS components (HPr, E_I, and E_{II}) can be estimated from the rate of sugar phosphorylation of the PTS if conditions are found where this rate is approximately proportional to the concentration of the component under investigation. Since this rate generally will be a function of all three PTS components, measurements should be made at fixed concentrations of the two components not under investigation. Figure 8, presenting plots of phosphotransferase activity against HPr concentration, at fixed concentrations of E_I and E_{II}, shows that, although the above condition is fulfilled, the shape of the plots may vary considerably. This observation, by itself, implies that another component should be involved. To obtain more insight into this phenomenon, a detailed theoretical treatment of the shape of the curves in Figure 8 will be given here. This will be done on the basis of the tentative model in Scheme II, which, of course, is a simplification of the PTS but suffices to explain the complications encountered in Figure 8.

In Scheme II, the following assumptions are made.

(1) The reaction PEP + αMglc ⇌ Pyr + αMglc-6-P is catalyzed by a combination of three components (HPr, E_I, and E_{II}) which can be added separately to the reaction mixture. Generally HPr and E_I are used in pure form; E_{II} is added as a membrane fraction. The overall conversion is followed by measuring the αMglc-6-P concentration as a function of time. Since, in our experiments, the slope of these plots was constant for at least the first 10% of the αMglc conversion, it gives the initial rate of phosphorylation in the steady state, as plotted on the ordinate in Figure 8. This rate equals

$$v = \frac{d(\alpha\text{Mglc-6-P})}{dt} = k_4(E_{II}\text{:P-HPr})$$

The reactions

$$\text{HPr} + \text{PEP} \rightleftharpoons \text{P-HPr} + \text{Pyr}$$

and

$$\text{P-HPr} + \alpha\text{Mglc} \rightleftharpoons \text{HPr} + \alpha\text{Mglc-6-P}$$

catalyzed by E_I and E_{II}, respectively, operate according to

ping-pong mechanisms. However, if one of these, or both, would operate according to an ordered mechanism, the basic principles of the model in Scheme II would remain the same by substituting PEP:E_I for E_IP, PEP:E_I:HPr for E_IP:HPr, αMglc:E_{II} for E_{II}, and αMglc:E_{II}:P-HPr for E_{II}:P-HPr.

(3) The conversions of E_I to E_IP and $E_{II}P$ to E_{II} are fast compared with the other steps in Scheme II, implying that

$$e_I = (E_IP) + (E_IP{:}HPr) \quad (1)$$

$$e_{II} = (E_{II}) + (E_{II}{:}P\text{-}HPr) \quad (2)$$

$$p = (HPr) + (P\text{-}HPr) + (E_IP{:}HPr) + (E_{II}{:}P\text{-}HPr) \quad (3)$$

in which e_I, e_{II}, and p represent, respectively, the total concentrations of E_I, E_{II}, and HPr, added at zero time. This assumption is in line with the observations (not shown) that, under the conditions measured in Figure 8, the concentrations of PEP (5 mM) and αMglc (2.5 mM) appeared to be saturating, the apparent K_M for both substrates being lower than 1 mM.

Steady-State Approximation. If a steady state may be assumed in all E_I, E_{II}, and HPr complexes mentioned in eq 1–3, the relation between v, p, e_I, and e_{II} will be

$$\frac{p}{v} = \frac{1}{k_2}\left[1 + \frac{K_M{}^I}{(e_I - v/k_2)}\right] + \frac{1}{k_4}\left[1 + \frac{K_M{}^{II}}{(e_{II} - v/k_4)}\right] \quad (4)$$

in which $K_M{}^I = (k_{-1} + k_2)/k_1$ and $K_M{}^{II} = (k_{-3} + k_4)/k_3$. It should be noted that, in this formula, no assumptions are made whether p, e_I, or e_{II} is in excess with respect to the other two components. As a consequence, the usual assumptions made in Michaelis–Menten kinetics, namely, that the concentration of substrate added equals the free substrate concentration, do not hold. Therefore, the terms $(e_I - (v/k_2))$ and $(e_{II} - (v/k_4))$, which are equal to the steady-state concentrations of E_IP and E_{II}, respectively, appear in the right-hand side of eq 4. Furthermore, the question whether HPr should be regarded as a substrate or an enzyme is irrelevant for the derivation of eq 4. In fact, eq 4 is identical with the reciprocal rate equation of a ping-pong mechanism if HPr is considered to be an enzyme and E_IP and E_{II} are the substrates. In that case, HPr would catalyze the phosphoryl group transfer from E_IP to E_{II} via the PHPr intermediate. Thus, within the assumptions made for the model in Scheme II, eq 4 is the most general equation that describes the relationship between v and the three components HPr, E_I, and E_{II}, irrespective of their quality and quantity.

Theoretical Saturation Curve. In order to explain the curves in Figure 8, it is more convenient to consider p as a function of v, e_I, and e_{II}, as is rewritten in eq 5. Figure 9 shows how

$$p = \underbrace{\frac{K_M{}^I}{(k_2e_I/v - 1)}}_{p_1} + \underbrace{\frac{K_M{}^{II}}{(k_4e_{II}/v - 1)}}_{p_2} + \underbrace{\left(\frac{1}{k_2} + \frac{1}{k_4}\right)v}_{p_3} \quad (5)$$

a theoretical saturation curve in eq 5 is built up of three separate terms, p_1, p_2, and p_3, which according to eq 3 equal the concentrations of HPr, P-HPr, and the sum of the HPr:enzyme complexes, respectively. It should be noted that, for any given value of v, the contributions p_1, p_2, and p_3 have to be added in order to construct the v vs. p plot. The meaning of the separate terms, however, is more easily understood by writing v explicitly for each of them so that

$$v = \frac{k_2e_I}{(1 + K_M{}^I/p_1)} = \frac{k_4e_{II}}{(1 + K_M{}^{II}/p_2)} = \frac{k_2k_4}{(k_2 + k_4)}p_3 \quad (6)$$

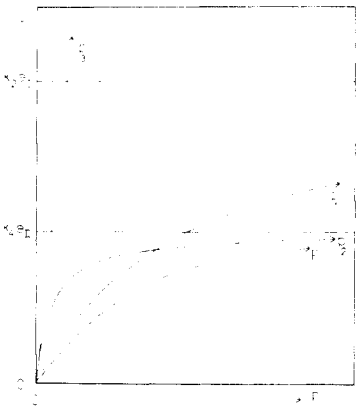

FIGURE 9: Theoretical plot of the rate of sugar phosphorylation (V) as a function of the HPr concentration (p), showing how the summation curve, P (- - -), appropriate to eq 5, is built up from the three separate terms p_1, p_2, and p_3.

is obtained. It follows that the theoretical saturation curve consists of two hyperbolas and a straight line. The slope of the straight line (v vs. p_3) is a function of the turnover numbers k_2 and k_4 of e_I and e_{II}, respectively. The hyperbolas describe the saturation of e_I and e_{II} by p_1(HPr) and p_2(P-HPr), respectively, and are limited at high values of p by the asymptotes $v = k_2e_I$ and $v = k_4e_{II}$. The summation curve (P) is limited, at high values of p, by the asymptote of the hyperbola which yields the lowest rate ($v = k_4e_{II}$ in Figure 9). However, depending on the relative values of $K_M{}^I$ and $K_M{}^{II}$, the other hyperbola (that for e_I in Figure 9) may provide the main contribution to the summation curve, at low values of p.

From the above tentative model, the following conclusions may be drawn. (1) The theoretical curve of saturation by HPr generally approximates a hyperbola, which differs from the orthogonal hyperbola usually found for simple Michaelis–Menten kinetics. (2) Situations may exist in which the saturation curve, measured at fixed e_I and e_{II}, reflects, partly, the interaction of HPr with E_I and, partly, that of P-HPr with E_{II}. (3) Although complications, as mentioned under point 2 may occur, they never cause the saturation curve to become a sigmoid. (4) The saturation curves approximate a linear relationship between v and p at subsaturating concentrations of p, where v is so low that $v \ll k_2e_I$ and $v \ll k_4e_{II}$. Then eq 5 reduces to

$$p = \left[\frac{1}{k_2}\left(1 + \frac{K_M{}^I}{e_I}\right) + \frac{1}{k_4}\left(1 + \frac{K_M{}^{II}}{e_{II}}\right)\right]v \quad (7)$$

The last conclusion gives the conditions where the relative concentration of HPr can be estimated from the rate of sugar phosphorylation of the PTS. The proportionality factor between v and p in eq 7 is constant if v is measured at fixed E_I and E_{II} concentrations. Conclusions 2 and 3 imply that, if a sigmoidal curve is found, as, for instance, in Figure 8 with pure HPr, the binding of HPr to E_I or P-HPr to E_{II} or both should be cooperative. Since, in that case, $K_M{}^I$, $K_M{}^{II}$, or both change depending on the concentration of (P)HPr, the proportionality factor in eq 7 never will be a constant. However, in the presence of a sufficient amount of an effector, which stabilizes one conformation of the enzyme, the K_M and, therefore, also the proportionality factor would be a constant.

Isolation of HPr. The procedure described in this paper is faster than the procedures thus far published for *E. coli* and *S. aureus* HPr (Anderson et al., 1971; Jennings & Smith, 1973; Greenwood, 1970; Beyreuther et al., 1977) since only two column chromatographies are involved. This improvement

Table I: Purification of HPr[a]

fraction	protein content (g)	purificn	recovery (%)
crude cell extract	4	1	100
protamine sulfate	3.6	1	90
DEAE pool	0.05	60	75[c]
concd DEAE pool	0.05	60	50[c]
Sephadex G-75 pool	0.007	286	34[c] (50)[b]

[a] HPr was purified from 100 g (wet weight) of *E. coli* K235. Details of the purification procedure are described in the text. The recovery was determined from the data in Figure 8 as described under Discussion. [b] Obtained from the preparation in Figure 8, recombined with saturating amounts of α1-6 glucan. [c] The two peaks from Figure 1B, recombined.

originates in the more highly resolved chromatogram from the DEAE column when gradient elution is employed. However, the impure HPr preparation obtained after batchwise elution from DEAE and subsequent Sephadex G-75 chromatography could be purified by rechromatography on DEAE-cellulose (not shown) resulting in a single HPr peak, pure by the criteria shown in Figure 3.

Recovery of HPr. The concentrations of the HPr preparations, plotted on the abscissa in Figure 8, were obtained as follows: (1) that of pure HPr was determined by Lowry's method; (2) the concentrations of HPr in the earlier stages of the isolation were computed from the concentration of pure HPr on the basis of an assumed 100% recovery per purification step. The latter values are, therefore, underestimated. In principle, it should be possible to estimate from the measurements in Figure 8 the real concentration of HPr in each preparation (and therefore its recovery) by adapting the unit on the abscissa for each particular HPr preparation so that its hyperbola would fit with that of pure HPr. From the theoretical treatment above (see conclusion 4), it follows that, in practice, fitting of the slopes of the straight portions of the hyperbola, determined at low values of PTS activity and HPr concentration, already is satisfactory for this purpose. This implies that the recovery of HPr in the different stages of isolation can be estimated directly from Figure 8 by fixing the above mentioned slope for crude cell extract at 100% and determining the slopes of the other preparations relative to it. However, if this method as such were applied to Figure 8, its results would be obviously misleading since the curves deviate increasingly from hyperbola, the purer the HPr. This complication, due to the removal of the sugar polymer, was avoided by measuring the curve of pure HPr in Figure 8 also in the presence of a saturating amount of the sugar (see theoretical treatment above, conclusions 2 and 3). The data obtained by this method are compiled in Table I.

The purification factor of the isolation procedure described in this paper (286 in Table I) is about as high as found with Anderson's procedure (301 of Anderson et al., 1971), but the recovery is higher. The 50% recovery is a reliable value if a loss of 15% per purification step is taken into account for a total of four steps. In fact, the recovery should be higher since, in Figure 8, α1-6 glucan does not completely restore the hyperbola. The 15% loss after concentration of the DEAE pool is artificial, due to the destruction of α1-6 glucan by bacterial growth. Even the 75% recovery of the DEAE pool is probably underestimated since the two peaks from the DEAE column, sugar rich and sugar poor, were recombined before the measurement of PTS activity in Figure 8. The yield, by the current method (7 mg of HPr from 4 g of protein in crude cell extract), is consistent with the 15 mg/8 g determined for *S. aureus* (Beyreuther et al., 1977) and 50% higher than the yield that can be calculated from Anderson's results with *E. coli* (20 mg from 17 g of protein) (Anderson et al., 1971). However, the latter difference is probably due to an editorial fault in the manuscript (Anderson et al., 1971) since his 17 g of protein from 100-g cells, wet weight, is an unusually high value.

Origin and Role of α1-6 Glucan. The data presented in this report are the first demonstration that α1-6 glucan polysaccharide can be found in soluble *E. coli* extracts. The origin of this polysaccharide is not known. Except for the French press step used to rupture the cells, all other handlings of the membrane and cell wall components are very gentle. It seems unlikely, therefore, that the material was originally an integral membrane structural component. It is possible that it is an exopolysaccharide coming from the capsule or slime layer which is partially degraded upon rupturing the cells. α1-6 glucan, however, has not been observed previously among *E. coli* exopolysaccharides (Sutherland, 1977). One trivial explanation is that the polymer is a degradation product of Sephadex, a cross-linked polymer of α1-6 glucans. However, proton NMR showed that the same polysaccharide was present in the HPr pool from the DEAE column (see Figure 1B) which had never been in contact with Sephadex.

The isolation procedure presented above indirectly provides some insight into the origin of the polysaccharide. It is retarded on DEAE-cellulose, while most of the sugar in the crude cell extract is not retarded. This could be explained assuming the polysaccharide carried a negatively charged glucose derivative (e.g., glucose-P) which binds to DEAE. Another explanation is that the retardation on the first DEAE column reflects a noncovalent or labile covalent binding of the polysaccharide to protein which, in turn, binds to DEAE. Obviously, HPr is the most likely protein candidate. On DEAE (Figure 1B), HPr elutes in two peaks, only one of which contains sugar. This elution behavior is not due to heterogeneity in the amino acid composition of HPr as found by Anderson et al. (1971) since (1) on rechromatography over DEAE-cellulose, the pure, sugar-free HPr eluted as a single peak at about 60 mM KCl, the position of the sugar-free peak in Figure 1B; (2) the purified HPr gave a single band on all polyacrylamide gel electrophoresis (see Figure 3).

The elution profile of the Sephadex G-75 column also indicates a binding of α1-6 glucan to HPr. In Figure 4, a portion of the HPr is retarded, eluting as a shoulder after the main HPr peak and overlapping the α1-6 glucan peak. Glucan-free HPr, however, elutes as a single symmetrical peak (see Figure 2B). Altogether, these results suggest a weak binding of α1-6 glucan to HPr.

At the present time, we do not have a clear understanding of the role of the polysaccharide in the PTS. There are, nevertheless, a number of possibilities. (1) The sugar could be originally covalently bound to HPr. The possibility of HPr as a glycoprotein is not unrealistic in light of the osmotic shock experiments of Kundig et al. (1966) which indicate that HPr may be located in the periplasmic space. Viewed from this perspective, the results of our reconstitution studies are quite reasonable. As we reported, the addition of pure α1-6 glucan to pure HPr only partially restored the hyperbola normally found in HPr concentration dependent activity measurements by using impure HPr from crude cell extract. If HPr is a glycoprotein, the polysaccharide will be covalently bound to the HPr in the crude cell extract and, using a reconstituted system where the components are not covalently bound, we would expect a less efficient system and lower activity. (2)

The polysaccharide could also originate in the membrane where it may have a specific role in the binding of P-HPr to membrane-bound E_{II}. This would correlate with its apparent activation effect which we find in the phosphotransferase activity measurements. (3) If one assumes that the α1–6 glucan is a form of sugar storage not previously detected, one could suggest that the polysaccharide may function as a mechanism for controlling the activity of the PTS. By considering that the PTS appears to be involved in regulating a number of other systems (adenylate cyclase, transport of non-PTS sugars (Saier, 1977)), it is possible that the polysaccharide has a more general role in the control of these processes. (4) The polysaccharide could be an intermediate product of the sugar transport process itself. Its discovery, then, would suggest that the PTS might transport sugar in the form of long polymers. In this respect it is tempting to speculate whether the structure of the polymer, being an α1–6 helix, has a special function. α1–6 helices should be much longer that the usual α1–4 amylose helices which are involved in the storage of sugar. These various possibilities are currently under investigation.

Recent experiments isolating HPr from *Salmonella typhimurium* grown and harvested under a variety of conditions consistently result in an HPr preparation which contains the α1–6 glucan homopolymer.

Acknowledgments

We wish to gratefully acknowledge the expert technical assistance of R. Ten Hoeve-Duurkens and the generosity of the Gist en Spiritus factory, Delft, The Netherlands, for the large-scale fermentation of *E. coli*. The gas chromatographic and mass spectral analyses have been performed in the organic chemistry department at the University of Utrecht. We are indebted to Drs. J. F. G. Vliegenthart and J. P. Kamerling for these analyses. The generosity of Dr. P. Postma in supplying the *Salmonella typhimurium* pts mutants is gratefully acknowledged. Lastly, we wish to acknowledge Dr. R. Kaptein and K. Dijkstra for their technical assistance with the NMR spectrometer.

References

Anderson, B., Weigel, N., Kundig, W., & Roseman, S. (1971) *J. Biol. Chem. 246*, 7023–7033.
Beyreuther, K., Raufuss, H., Schrecker, O., & Hengstenberg, W. (1977) *Eur. J. Biochem. 75*, 275–286.
Cirillo, V. P., & Razin, S. (1973) *J. Bacteriol. 113*, 212–217.
Fiske, C. H., & SubbaRow, Y. (1925) *J. Biol. Chem. 66*, 375–381.
Greenwood, C. T. (1970) in *The Carbohydrates* (Pigmon, W., & Horton, D., Eds.) Vol. IIB, pp 471–513, Academic Press, New York.
Jennings, H. J., & Smith, I. C. P. (1973) *J. Am. Chem. Soc. 95*, 606–608.
Kundig, W., & Roseman, S. (1971a) *J. Biol. Chem. 246*, 1393–1406.
Kundig, W., & Roseman, S. (1971b), *J. Biol. Chem. 246*, 1407–1418.
Kundig, W., Kundig, F. D., Anderson, B. F., & Roseman, S. (1966) *J. Biol. Chem. 241*, 3243–3246.
Lowry, O. H., Rosebrough, N. J., Farr, A. L., & Randall, R. J. (1951) *J. Biol. Chem. 193*, 265–275.
Postma, P. W. (1976) *FEBS Lett. 61*, 49–53.
Postma, P. W., & Roseman, S. (1976) *Biochim. Biophys. Acta 457*, 213–257.
Robillard, G. T., Dooijewaard, G., & Lolkema, J. (1979) *Biochemistry 18* (first of three papers in this issue).
Roseman, S. (1969) *J. Gen. Physiol. 54*, 138s–180s.
Saier, M. H., Jr. (1977) *Bacteriol. Rev. 41*, 856–871.
Sutherland, I. W. (1977) in *Surface Carbohydrates of the Prokaryotic Cell* (Sutherland, I., Ed.) pp 27–96, Academic Press, New York.
Winzler, R. J. (1955) *Methods Biochem. Anal. 2*, 279–311.

Escherichia coli Phosphoenolpyruvate Dependent Phosphotransferase System. NMR Studies of the Conformation of HPr and P-HPr and the Mechanism of Energy Coupling†

G. Dooijewaard, F. F. Roossien, and G. T. Robillard*

ABSTRACT: ^{1}H and ^{31}P nuclear magnetic resonance investigations of the phosphoprotein intermediate P-HPr and the parent molecule HPr of the *E. coli* phosphoenolpyruvate dependent phosphotransferase system (PTS) show that HPr can exist in two conformations. These conformations influence the protonation state of the reactive histidine residue, thereby determining the reaction pathway in the phosphoryl group transfer step. A general mechanism is proposed for the energy-coupling process in the PTS.

The transport of sugars by the bacterial phosphoenolpyruvate dependent phosphotransferase system is coupled to the energy source, phosphoenolpyruvate, via a series of phosphoryl group transfer steps involving phosphoenzyme intermediates (Roseman, 1969; Postma & Roseman, 1976; Hengstenberg, 1977).

$$\mathrm{PEP}^1 + \mathrm{E_I} \overset{\mathrm{Mg^{2+}}}{\leftrightarrow} \mathrm{P\text{-}E_I} + \text{pyruvate}$$

$$\mathrm{P\text{-}E_I} + \mathrm{HPr} \leftrightarrow \mathrm{P\text{-}HPr} + \mathrm{E_I}$$

$$\mathrm{P\text{-}HPr} + \mathrm{F_{III}} \leftrightarrow \mathrm{P\text{-}F_{III}} + \mathrm{HPr}$$

† From the Department of Physical Chemistry, University of Groningen, Paddepoel Groningen, The Netherlands. *Received January 22, 1979.* This research and the 360-MHz NMR facility at the University of Groningen have been supported by the Netherlands Foundation for Chemical Research (S.O.N.) with financial aid from the Netherlands Organization for the Advancement of Pure Research (Z.W.O.).

[1] Abbreviations used: PEP, phosphoenolpyruvate; PTS, phosphoenolpyruvate dependent phosphotransferase system; DSS, 2,2-dimethyl-2-silapentane-5-sulfonate; DTT, dithiothreitol; P (as in P-histidine), phospho.

0006-2960/79/0418-2996$01.00/0 © 1979 American Chemical Society